Materials Research Express

PAPER

Adsorption of fluoride from aqueous solution using biochar prepared from waste peanut hull

To cite this article: Pawan Kumar *et al* 2019 *Mater. Res. Express* **6** 125553

Materials Research Express

PAPER

Adsorption of fluoride from aqueous solution using biochar prepared from waste peanut hull

RECEIVED
30 September 2019

REVISED
13 January 2020

ACCEPTED FOR PUBLICATION
16 January 2020

PUBLISHED
29 January 2020

Pawan Kumar, Anuj Kumar Prajapati, Shobhit Dixit and Vijay Laxmi Yadav

Department of Chemical Engineering and Technology, Indian Institute of Technology, (Banaras Hindu University), Varanasi 221005, India

E-mail: vlyadaviitbhu2014@gmail.com

Keywords: adsorption, low cost adsorbent, peanut hull, Fluoride removal

Abstract

In the present study, cost-effective biochar was prepared from waste peanut hull powder (PHP) and utilized as an adsorbent for the removal of fluoride from aqueous solution by adsorption experiment. Different techniques such as FTIR, BET, SEM, and EDX were used to analyze the surface functionality, surface area, surface morphology, and elemental composition of PHP biochar adsorbent, respectively. The batch experiments were carried out to optimize various effecting parameters like initial pH, contact time, PHP biochar adsorbent dose, initial concentration of Fluoride ion in solution, and reaction temperature. The maximum removal efficiency of PHP biochar adsorbent was 88.21% for the 10 mg l^{-1} fluoride concentration at pH 7 with 8 g l^{-1} biochar dose. For the isotherm study, adsorption equilibrium data were linearly fitted with experimental data to explain the adsorption process. Thermodynamic analysis results show that the adsorption of Fluoride onto PHP biochar adsorbent was a spontaneous, exothermic, and feasible process under experimental condition. Kinetic study of the adsorption process reveals that the pseudo-second-order model best fitted with experimental data as compared to the pseudo-first-order model.

1. Introduction

Fluoride is one of the elements present in groundwater. However, fluoride is an essential element for living bodies, but in more than an appropriate limit, it can create harmful effects on health and the environment. A large population in the world is suffering from fluoride contamination specifically in rural areas of developing countries [1, 2]. It is reported that almost 200 million people in Asian and African countries are facing dental and skeleton fluorosis issues due to fluoride contamination [3]. In rural India, the availability of treated water is very limited, and the population living in that regime is dependent on direct sources of untreated water. Above 400 million people are at the risk of fluoride contamination and 66 million among them are facing fluorosis in India [4].

In recent years, this problem has drawn the significant interest of many researchers to develop various technologies like photo catalytic-degradation, ozonation, adsorption, precipitation, membrane separation, bioremediation, coagulation, etc to treat groundwater to make it safe for drinking [5]. Among the so many available technologies for water cleaning and purification, adsorption is one of the most common and efficient technology for the removal of fluoride from groundwater because of its advantages of simple design, smooth operation and low-cost requirement [6]. The efficiency of these techniques mainly depends on adsorbents. Continuous research is going on for decades to study the effectiveness of numerous low cost adsorbent which is locally and naturally available [7].

Many different types of adsorbent materials such as Fly ash [8], bone char [9], furnace slag [10], modified alumina [11] and many more had been studied and reported for fluoride removal from aqueous medium. Agricultural waste-based adsorbents have their advantage of negligible cost, availability and eco-friendliness. Some of the plant-based adsorbents like orange waste [12], rice straw [13], palm shell waste [14], manihotesculenta [15], jamun seed [16], etc have been studied recently by various investigators and reported for

fluoride removal from water with different degrees of success. However, there was no reported literature on adsorption of fluoride ions onto the peanut hull powder biochar, which gave motivation to this study.

In the present work, effective and low-cost biochar was prepared by pyrolysis of peanut hull shell powder (PHP), which was used as an adsorbent to remove fluoride ions from aqueous solution. Pre-prepared PHP biochar adsorbent was characterized by different techniques such as FTIR, BET, HRSEM and EDX, to know their physio-chemical and surface properties. The adsorption of fluoride on the PHP biochar adsorbent was carried out in batch experiment mode, using differential operation conditions such as a change in initial pH, conduct time, initial fluoride concentrations, PHP biochar dose, and temperature. Equilibrium data were linearly fitted with the Langmuir and Freundlich models to describe the adsorption process. For the cost estimation, the kinetic model analysis was also done in this research paper by two generalized models such as pseudo-first-order and pseudo-second-order model. Besides this, the thermodynamic analysis was also discussed in the present study to know the spontaneous nature and flexibility of the fluoride adsorption onto PHP biochar adsorbent.

2. Materials

2.1. Chemicals, reagents and experimental equipment

Sodium fluoride, sodium hydroxide, hydrochloric acid were of pure analytical grade. Sodium fluoride was purchased from Sigma-Aldrich, USA and sodium hydroxide, hydrochloric acid were purchased from Sisco Research Laboratories Ltd, Mumbai, India. The deionized water was used in all experiments.

Various experimental equipment such as hot air oven (S M S I Pvt. Ltd, India), NSW-104 split tubular furnace single zone (Narang ScientificWorks Pvt. Ltd, India), pH meter (LI 120, Elico India) and orbital shaker incubator (model NSW-256 of company NSW, India) were used for experiments.

2.2. PHP biochar adsorbent preparation

Waste peanut shell was collected from the local market of Varanasi city, Uttar Pradesh, India. It was washed with distilled water to remove the dust and other impurities and then dried at 80 °C in a hot air oven. After drying, it was grounded in a grinder to obtain the powder. The peanut shell powder was then sieved between 80–120 mesh and stored in an airtight container for further use. For the preparation of PHP biochar, 10 g of sieved peanut powder was pyrolyzed in a tubular reactor with a limited supply of nitrogen gas with a flow rate of 150 ml min^{-1} at 400 °C for 1 h [17]. After pyrolysis, the biochar sample was cooled in nitrogen gas flow. After that, the biochar sample was again ground and sieved with the help of grinder and 200 mesh sieve, respectively. The obtained biochar was called PHP biochar. The obtained PHP biochar was stored in an airtight container for future use.

3. Characterization and experiment method

3.1. Characterization of PHP biochar

The high-resolution scanning electron microscope (HRSEM) was used to visualize the morphology of the prepared adsorbent. All the analysis was done using instrument Nova Nano SEM 450, FEI Company of USA (S E A) PTE, Ltd Since the sample is non-metallic, it was coated with gold before observation. Energy-dispersive x-ray spectroscopy (EDS) was used to verify the presence of carbon and oxygen ions in an untreated and fluoride-treated sample of the adsorbent. The surface area was measured by using BELLSORP MAX II & BELCAT-II, Microtrac BEL Corp, JapanBET surface area analyzer. Fourier transform infrared spectroscopy (FTIR) study was done to know functional groups present in adsorbent using Nicolet iS5, THERMO Electron Scientific Instruments LLC. Fluoride concentration in aqueous solutions was determined by spectrophotometric analysis using SL-210 ElICO UV–vis spectrophotometer at an absorbance value of 540 nm by using SPADNS method. Reagent solution of SPADNS i.e. sodium 2-(parasulphophenylazo)-1,8-dihydoxy-3,6-naphthalene disulphonate and zirconium is a red coloured complex which changes colour when it reacts with fluoride. The change in concentration of SPADNS-Zirconium solution causes a change in the transmittance of light, which is detected by the instrument.

3.2. Adsorption experiments

Batch experiments were carried out to understand the adsorption of fluoride on PHP biochar adsorbent. For kinetic studies, the desired concentration of fluoride samples was taken 200 ml flask with 50 ml fluoride solution, and 0.4 g PHP biochar adsorbent was added in solution. Then the samples were placed in an orbital shaker incubator at 25 °C temperature with 160 rpm speed of shaker. After that, samples were taken out from shaker at a different-different time interval, and samples were filtrated with the help of the Whatman filter paper. The residual fluoride concentration was measured by UV–vis spectrophotometer at 540 nm wavelength. The

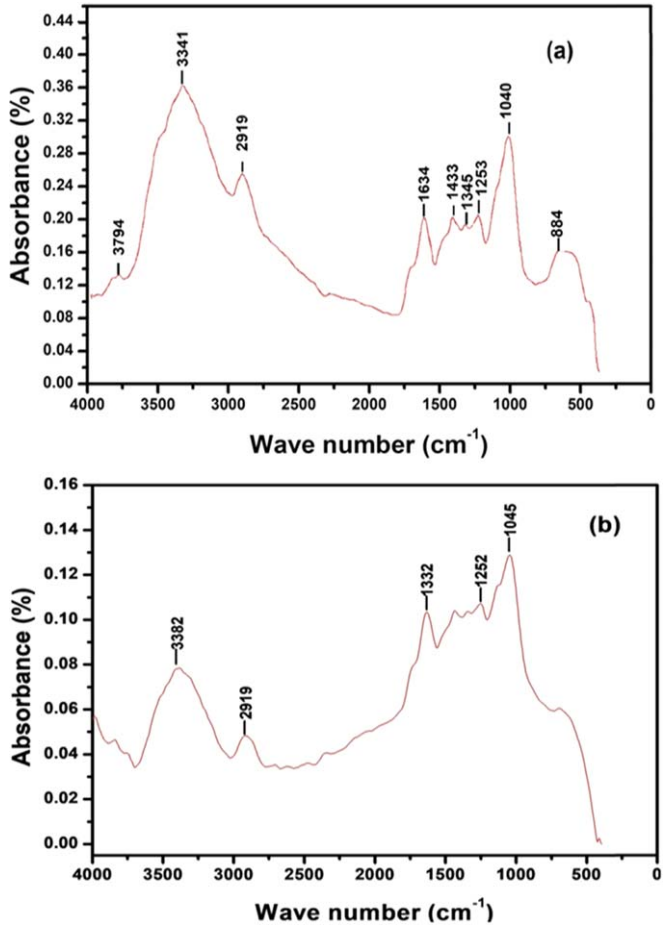

Figure 1. FTIR spectra of (a) PHP biochar and (b) Fluoride treated-PHP biochar.

effect of pH on the fluoride removal efficiency of the PHP biochar adsorbent was investigated by adjusting pH up to 2–11 with the help of 0.1 M HCl and 0.1 M NaOH solution. The effect of concentration on removal efficiency of PHP biochar was investigated with 8 and 10 g biochar dose with 10 to 50 mg l^{-1} concentration of fluoride. The effect of adsorbent dose was also observed using the adsorbent amount from 2–14 g l^{-1}. An effect of temperature on adsorption of fluoride onto PHP biochar was also observed by varying bath temperature from 25 °C–45 °C for 10 mg l^{-1} concentration of fluoride solution with 8 g PHP biochar adsorbent dose. The equations (1) and (2) are used to calculate the adsorption capacity of PHP biochar (mg g^{-1}) and removal percentage of fluoride, respectively [17]:

$$\mathbf{q_e(mg/L)} = \frac{(\mathbf{C_o^F} - \mathbf{C_e^F}) \times \mathbf{V}}{\mathbf{m}} \quad (1)$$

$$\%\ \mathbf{Removal\ of\ fluoride} = \frac{(\mathbf{C_o^F} - \mathbf{C_e^F}) \times 100}{\mathbf{C_o^F}} \quad (2)$$

where, C_o^F and C_e^F are the initial and equilibrium concentration of fluoride in solution (mg l^{-1}), respectively. V and m are the volume of solution (L) and mass of PHP biochar adsorbent (g), respectively.

4. Result and discussion

4.1. Characterization of PHP and fluoride-treated biochar adsorbent

Fourier transform infrared spectroscopy (FTIR) is the most important technique for determining functional groups, which are present on a sample. Figure 1 illustrates the FTIR spectra of PHP biochar and fluoride-treated biochar. Two strong absorbance peaks were present on the PHP biochar at 3794 and 3341 cm^{-1}, which was assigned to –OH stretching due to the presence of phenol, alcohol, and water vapor [18]. A low-intensity absorbance peak was present at 2919 cm^{-1}, which can be assigned to C–H stretching due to alkanes [19]. The absorbance peak at 1634 and 1433 cm^{-1} can be attributed to unsaturated alkene and carboxylate anion of C=O stretching, respectively [19]. The absorbance peak at 1345 and 1253 cm^{-1} corresponds to –C–H stretching and

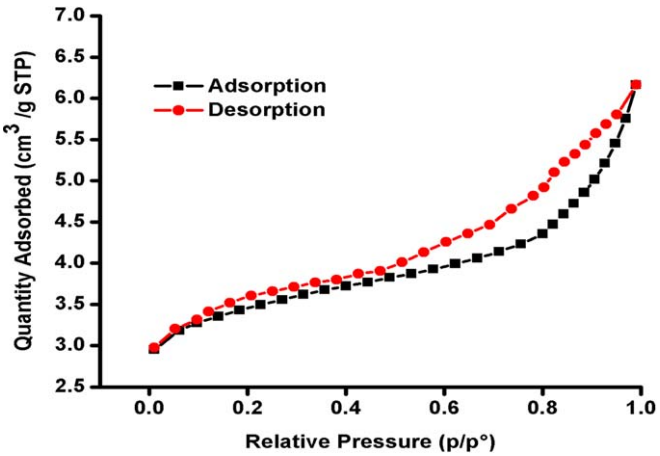

Figure 2. N_2 adsorption-desorption isotherm curve for PHP biochar.

C–N stretching vibration due presence of alkenes and amine, respectively [20]. A strong absorbance peak was observed at 1040 cm^{-1}, which can be assigned to C–O stretching vibration due to aldehyde and alcohol groups [17]. It is seen in figure 1 that after adsorption of fluoride, some peaks intensity was reduced and shift from their original position, which confirmed that adsorption of fluoride occurred on the PHP biochar adsorbent.

BET study was done for surface area analysis of PHP biochar adsorbent. BET surface area and pore volume of PHP biochar was 98.2 $m^2\ g^{-1}$ and 0.173 $cm^3\ g^{-1}$, respectively. The N_2 adsorption-desorption curve for PHP biochar adsorbent was illustrated in figure 2. It can be seen from the figure that the isotherm curve of PHP biochar can be classified as type II with H4 type hysteresis loop in the high-pressure region ($0.6 < p/p_o > 1$), which suggested multilayer adsorption and the presence of mesopores and macropores [18]. A very slow N_2 adsorption rate (2.8 to 3.5 $cm^3\ g^{-1}$ STP) occurred on the PHP biochar surface at the low-pressure region ($p/po > 0.2$) suggested that the number of micropores on the biochar surface was lesser in quantity, which was also confirmed by the SEM image. The N_2 adsorption rate at the medium pressure range was almost constant ($0.3 < p/po > 0.6$), which behaved like multilayer sorption. The N_2 adsorption rate was dramatically increased in the pressure range ($0.6 < p/po > 1$), due to the presence of a large number of macropores in the PHP biochar sample.

SEM analysis is an important technique to study the surface morphology of samples [14, 21–24]. SEM images of PHP biochar and fluoride-treated PHP biochar was shown in figure 3. The SEM image of PHP biochar shows a heterogeneous and irregular surface with a large number of irregularly shaped pits that are macro-sized. The SEM image of the treated biochar after the adsorption of fluoride ions shows a smooth and regular surface, and a minimal number of pits remain on the treated biochar surface.

EDX analysis is an important technique to determine the elements present in a sample. The EDX analysis of PHP biochar and fluoride-treated PHP biochar was shown in figure 4. The EDX results of PHP biochar show the presence of carbon, oxygen, and calcium are central elements in PHP biochar. On the pyrolysis of raw PHP at low temperature, carbon and oxygen are the main elements in biochar due to the degradation of cellulose, hemicellulose, and lignin. Calcium occurred due to the presence of calcite in the pyrolyzed sample. After adsorption, EDX analysis of the fluoride-treated biochar reveals the presence of a fluoride element, which confirms that the adsorption of fluoride occurred on the surface of the PHP biochar [12, 20, 21, 25, 26].

4.2. Effects of contact time

Contact time is another parameter that affects the adsorption process. As the contact time is increased, adsorption also increases until all active sites on the adsorbent surface are used for adsorption and equilibrium is reached. Experiments were further done for treating 10 mg l^{-1} fluoride solution using 0.4 g PHP biochar at 25 °C and pH 7 for time intervals of 15 min until equilibrium was reached and it was observed that initially higher rate of removal occurred but as the time increased above 90 min, change in removal was relatively small. This can be seen in figure 5(a). This was because initially higher numbers of active sites were available for adsorption at the adsorbent surface [27]. There was no further removal occurred beyond 120 min which showed that adsorbent got completely saturated within 120 min and no further adsorption was possible due to the unavailability of active sites. So the optimum time for adsorption was found to be 120 min.

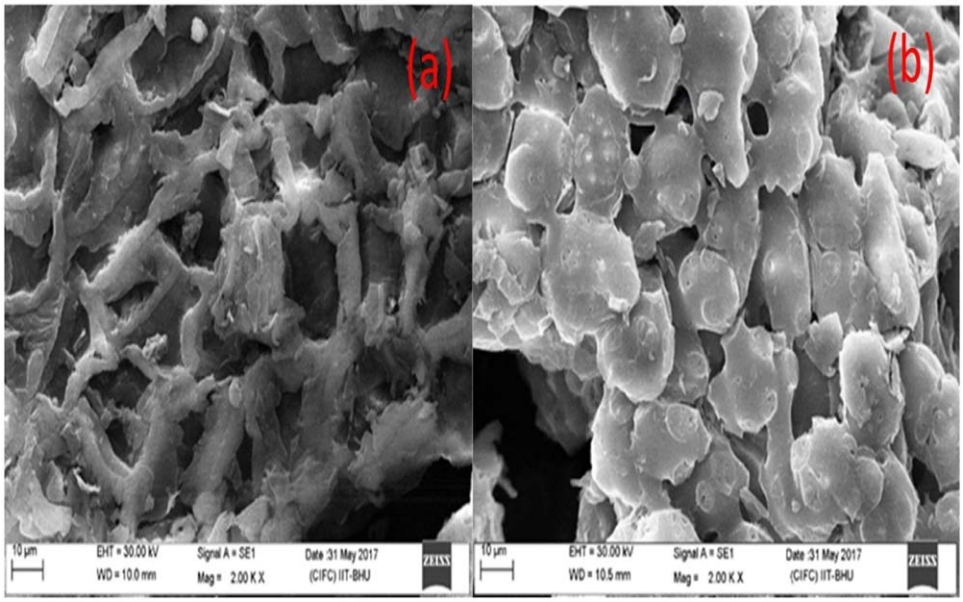

Figure 3. SEM images of (a) PHP biocharadsorbent and (b) Fluoride treated-PHP biochar.

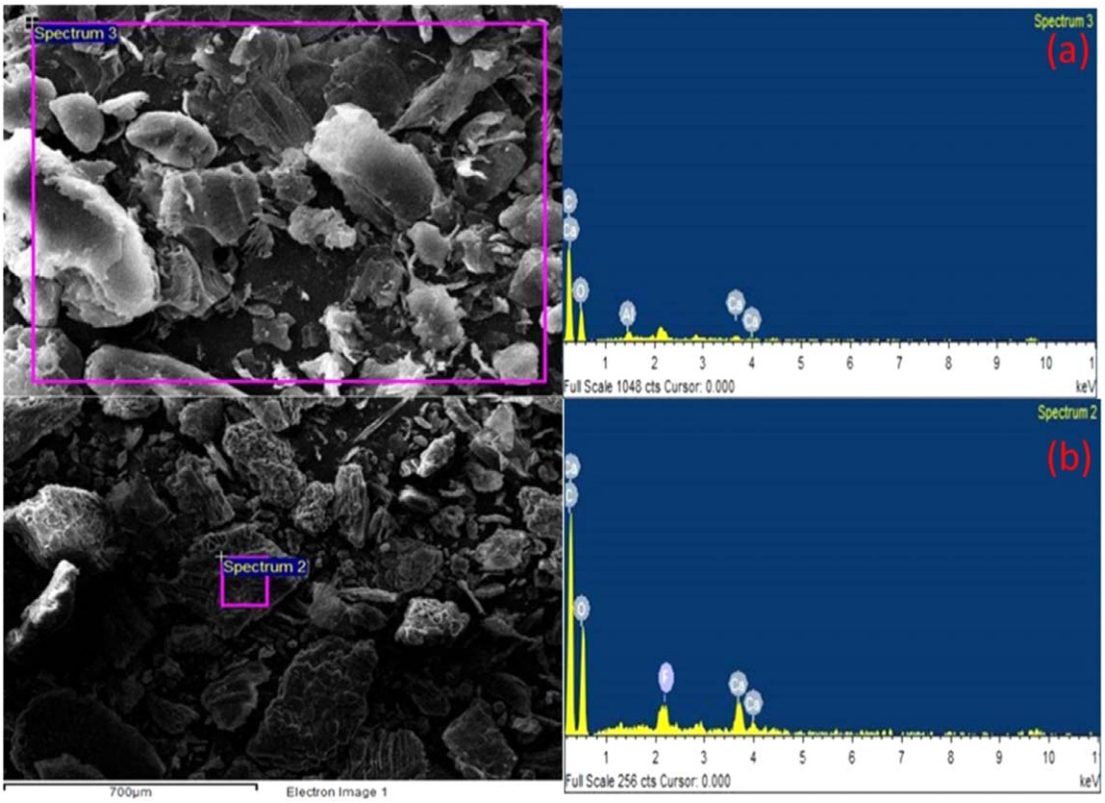

Figure 4. EDX analysis of (a) PHP biochar adsorbent and (b) Fluoride treated-PHP biochar.

4.3. Effects of pH

Since pH is an essential parameter for the adsorption process, it was necessary to optimize pH for maximum removal as pH can affect the surface charge on the adsorbents and adsorbate solution. Therefore, adsorption experiments were done for treating 10 mg l^{-1} fluoride solution between pH ranges of 2–11 using 0.4 g PHP biochar at 25 °C to study the effect of pH on fluoride removal. The pH of the solution was controlled using 0.1 M HCl and 0.1 M NaOH solutions. Experiments found that as the pH is increased from 2 to 7, fluoride removal was

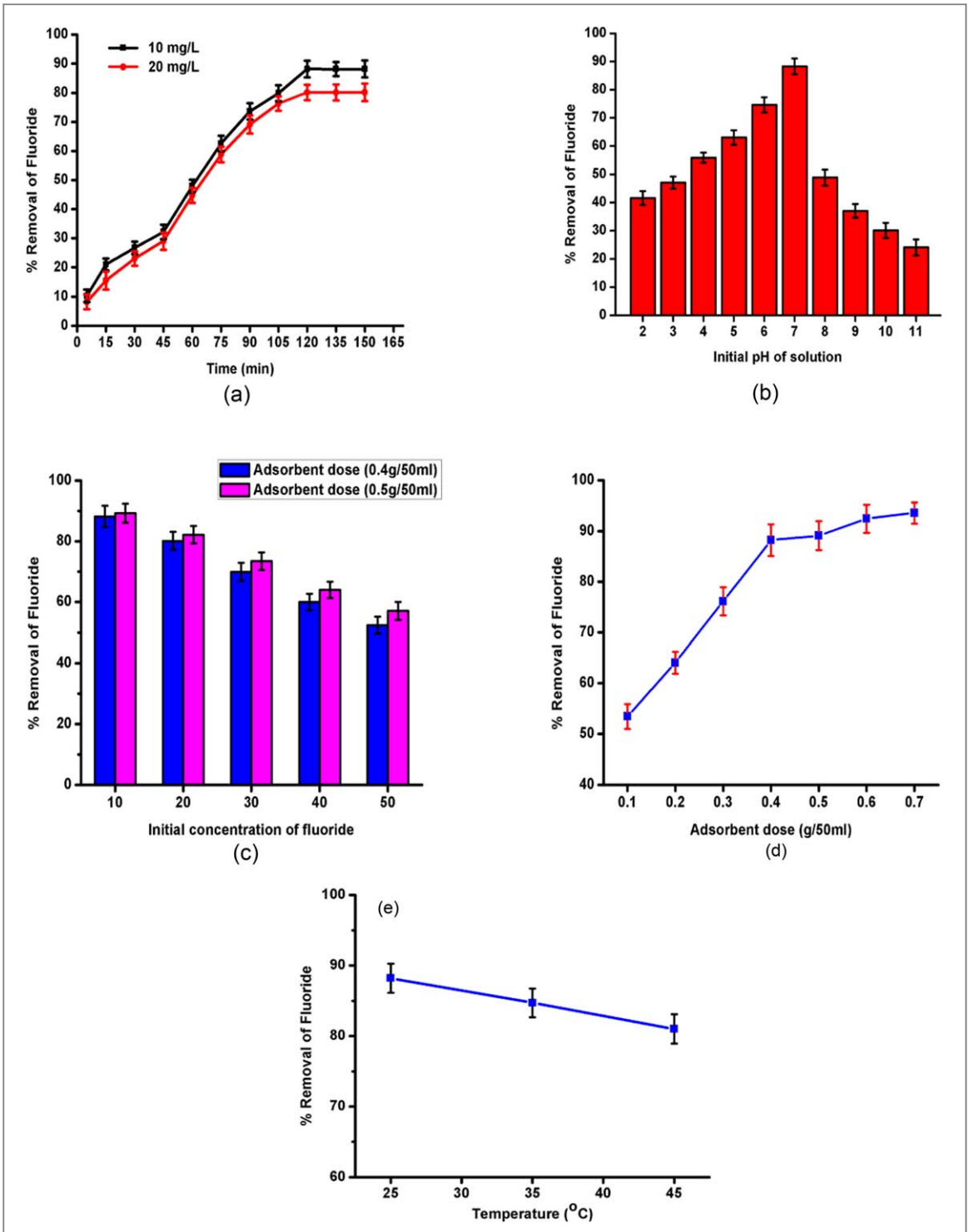

Figure 5. Effect of (a) contact time (b) initial pH, (c) initial concentration of Fluoride, (d) PHP biochar adsorbent dosage, (e) temperature on adsorption of Fluoride onto PHP biochar.

also increased from 41.55 to 88.22% and it started decreasing again from7 to 11 pH. Fluoride removal was increased from 2 to 7 pH because, in acidic medium, the formation of weak hydrofluoric acid takes place, which alters the adsorption fluoride ion onto the PHP biochar. Since in basic medium adsorbent surface, become negatively charged OH^- ions on the surface and fluoride ions were negatively charged. So an electrostatic repulsion was created between the adsorbent surface and fluoride ions. So that fluoride removal was decreased from pH 7 to 11. The maximum removal of fluoride of 88.2% was observed at pH seven, as shown in figure 5(b). Therefore no requirement of pH adjustment was found, and rest experiments were done on pH 7. Some other researchers also observed this optimum pH at 7 for their tests [28–30].

4.4. Effect of adsorbate concentration

Any adsorbent has a certain number of active sites, which are responsible for the adsorption of contaminant species from the solution. The effect of initial fluoride concentration was investigated by adding fixed amounts of biochar adsorbent onto solutions different fluoride concentrations of 10 and 20 mg l^{-1} at pH 7 and 25 °C. It can be seen from figure 5(d), on increasing fluoride concentration in solution the removal percentage was decreased. This may be due to the low availability of active sites in the solution. The removal percentage was reduced from 88.21 to 52.41 when fluoride concentration increased from 10 to 50 mg l^{-1} solution at constant biochar dose (8 g). Similarly, it was decreased from 89.25 to 57.88% when fluoride concentration increased from 10 to 50 mg l^{-1} solution at constant biochar dose (10 g).

4.5. Effects of adsorbent dose

Different range of adsorbent dose was also used to study the effect of adsorbent dose on fluoride removal from a concentration mixture of 10 mg l^{-1} fluoride at pH 7 and 25 °C and shown in figure 5(d). For this, the adsorbent dose of 2–14 g l^{-1} was used. The adsorption capacity of PHP biochar depends on the availability of active sites of functional groups and pores on its surface. A constant amount of adsorbent has a fixed number of active sites for adsorption, so as the amount of adsorbent was increased, there were more available active sites for fluoride adsorption on the surface of the adsorbent. Therefore removal of fluoride was also increased until the maximum possible removal was achieved. It was found that the removal percentage was varied from 53.46 to 91.09% for 2 g to 14 g biochar dosage, respectively. A similar mechanism was reported by Prajapati *et al* for As(III) removal [20].

4.6. Effect of temperature

The temperature has a substantial effect on the phenomenon of adsorption. After optimizing pH, adsorbent dosage and time, experiments were done on three different temperature conditions between 25 °C–45 °C at an interval of 10 °C, and as shown in figure 5(e), it was found that increasing temperature has shown a negative effect on the removal of fluoride ions because of the increase of Brownian motion and breaking of the intermolecular bond between PHP biochar and fluoride at higher temperatures. However, the reduction in removal at higher temperatures was not much high, and change of almost 7% was found at 45 °C, i.e., 81.02. So this adsorbent was still suitable for higher temperature conditions for treatment [31].

4.7. Adsorption isotherm

Adsorption isotherms play a crucial role in determining compatibility between adsorbent and adsorbate and provide knowledge of the effectiveness of adsorbent for removal of adsorbate from the mixture solution. There were different isotherms models such as the Langmuir, Freundlich, Dubinin-Radushkevich (D-R), and Brunauer-Emmer-Teller (BET) isotherm models were used by researchers to study the effectiveness of adsorbent [26, 27]. For the present study, Freundlich isotherm and Langmuir isotherm models were used for adsorption of fluoride ion onto PHP biochar, and experimental data were linearly fitted on models. The linear form of the Freundlich and Langmuir model equations are commonly written as [32],

$$\log q_e = \frac{1}{n}\log C_e + \log K_F \tag{3}$$

$$\frac{C_e}{q_e} = \frac{C_e}{q_m} + \frac{1}{q_m K_L} \tag{4}$$

where, C_e is equilibrium adsorbate concentration in the liquid phase (mg l^{-1}), q_e and q_m are adsorption capacity of adsorbent (mg g^{-1}) and maximum adsorption capacity of adsorbent (mg g^{-1}) calculate by Langmuir isotherm, respectively. K_L (l mg^{-1}) and K_F ($(mg^{1-1/n}\, L^{1/n})/g$) are the Langmuir and Freundlich constant, respectively $\frac{1}{n}$ is the heterogeneity factor constant.

The Langmuir constants K_L and q_m were calculated from the slope and intercept of the straight line, respectively as shown in figure 6(a). Similarly, the value of the Freundlich constant can be calculated by linear plotting graph of log q_e versus log Ce, and slope and intercept of the graph give values of constants as shown in figure 6(b). Constant value 'n' provides information about the degree of non-linearity between adsorption and solution concentration. If the value of 'n' is higher than 1, it shows that the process is purely physical, and if the value of 'n' is lesser than 1, it shows that the separation process involves some chemical changes also. From table 1, it was seen that the values of correlation coefficients (R^2) are almost equal to unity for the Langmuir isotherms model at all PHP biochar doses, suggesting that the Langmuir model best applied to the experimental data as compared to Freundlich isotherm. So, according to the Langmuir model, the adsorption of fluoride onto PHP biochar occurred by monolayer adsorption of the surface of biochar adsorbent. Table 1 shows that the value of n was greater than 1, which means that the lower value of 1/n would be less than 1, so it can be said that the adsorption process is feasible. The values of maximum Langmuir adsorption capacity were 3.665 mg g^{-1} and

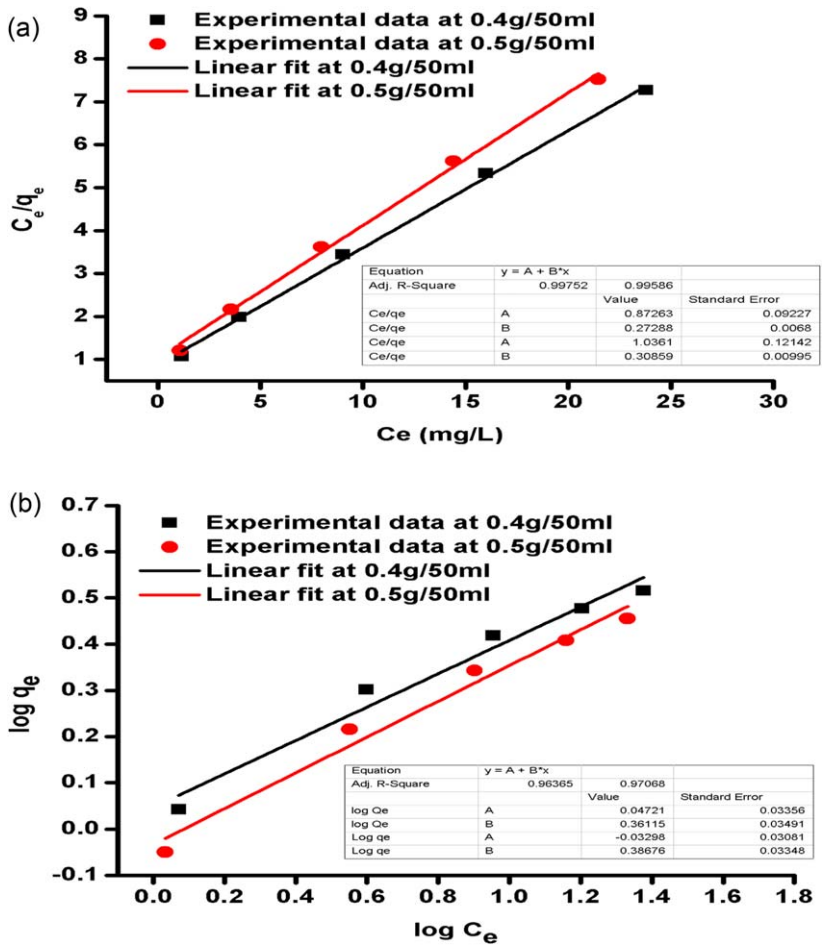

Figure 6. Fitting plots of isotherms model of (a) Langmuir,and (b) Freundlich isotherm for adsorption of Fluoride onto PHP biochar.

Table 1. Isotherm parameters value for adsorption of Fluoride onto PHP biochar.

	Operating condition		
Isotherm	**Parameter**	**0.4 g/50 ml**	**0.5 g/50 ml**
Langmuir	$\mathbf{q_{max}}$**(mg/g)**	3.665	3.241
	$\mathbf{K_L}$ **(L/mg)**	0.313	0.299
	$\mathbf{R_L}$	0.242	0.251
	$\mathbf{R^2}$	0.9975	0.9959
Freundlich	$\mathbf{K_F((mg^{1-1/n}\,L^{1/n})/g)}$	1.115	0.927
	n	2.769	2.586
	$\mathbf{R^2}$	0.9637	0.9706

3.241 mg/g for 0.4 g/50 ml and 0.5 /50 ml biochar dose, respectively. The adsorption capacity of Fluoride ions onto PHP biochar was compared with other adsorbents and tabulated in table 2.

4.8. Adsorption kinetics

Adsorption kinetics study is done to understand the adsorption mechanism, i.e., rate-determining step and mass transfer from solution to the adsorbent surface. In this study, two well-known kinetic models, the pseudo-first-order, and the second-order model was used to describe the adsorption of fluoride onto PHP biochar [17, 21]. Equations (5) and (6) represents the linear form of the pseudo-first-order, and the second-order model, respectively [21].

$$\log(q_e - q_t) = \log q_e - \frac{k_1}{2.303} * t \quad (5)$$

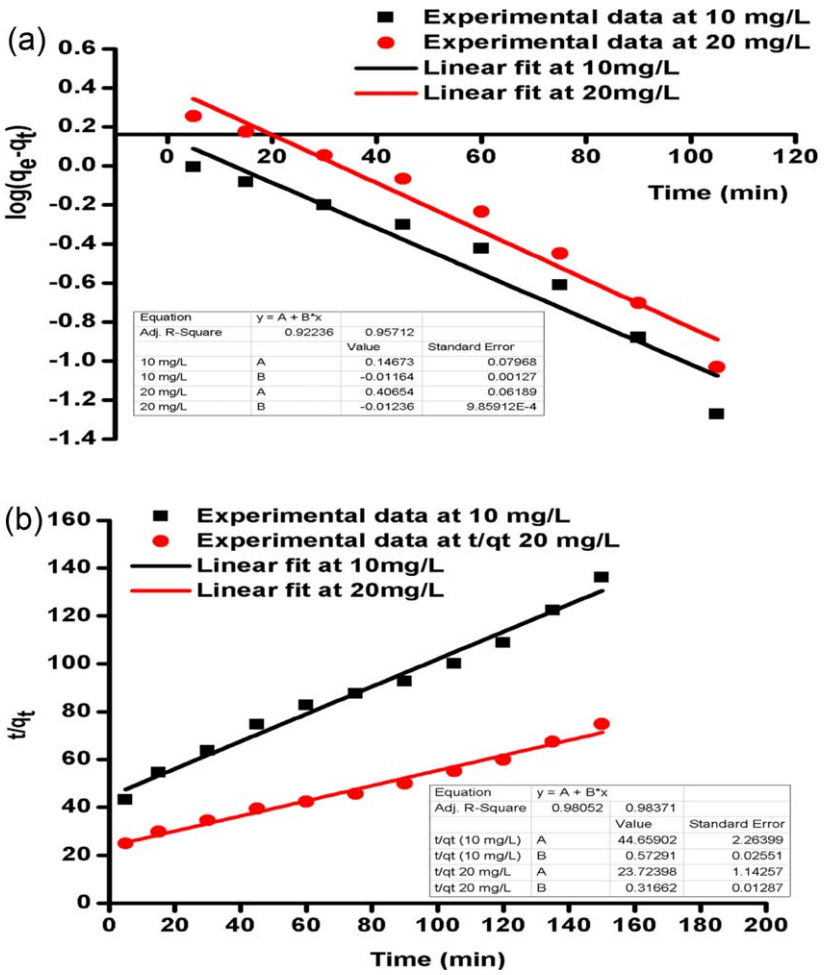

Figure 7. Fitting plots of kinetic model of (a) pseudo-first-order, and (b) pseudo-second-order for adsorption of Fluoride onto PHP biochar.

$$\frac{t}{q_t} = \frac{1}{K_2 q_e} + \left[\frac{1}{q_e}\right] * t \tag{6}$$

where, q_e and q_t are adsorption capacity for PHP biochar at equilibrium and time 't' (mg g^{-1}), respectively. K_1 and K_2 are rate constants for pseudo-first-order, and the second-order model, respectively. For fluoride concentrations of 10 mg l^{-1} and 20 mg l^{-1}, plots were made for log (q_e–q_t) against time (t) for the pseudo-first-order, as shown in figure 7(a). Similarly, for fluoride concentrations of 10 mg l^{-1} and 20 mg l^{-1}, data was plotted between t versus t/q_t for the pseudo-second-order, as shown in figure 7(b). The parameters reported in the models were calculated by the slope and intercept of the linear fitted plots of experimental data. According to correlation coefficients (R^2), as given in Table 3 the pseudo-second-order model was the best linear fitted with experimental kinetic data as compared to the pseudo-first-order model. Therefore, the rate-determining step for the adsorption of fluoride onto PHP biochar was chemisorption, and the $q3_e$ (adsorption capacity) was proportional to the number of active sites on the PHP biochar adsorbent.

4.9. Thermodynamic studies

Thermodynamic studies were performed to understand the chemical reaction change during adsorption and know the nature of energy involved in the adsorption process. The following equations calculated thermodynamic parameters such as a change in standard Gibbs free energy change (ΔG^0), change in standard entropy (ΔS^0) and change in standard enthalpy (ΔH^0) for the adsorption of fluoride onto PHP biochar:

$$\Delta G^0 = \Delta H^0 - T \times \Delta S^0 \tag{7}$$

$$\Delta G^o = -R \times T \times \ln K_{CF} \tag{8}$$

$$\ln (K_{CF}) = \frac{\Delta S^o}{R} - \frac{\Delta H^o}{R \times T} \tag{9}$$

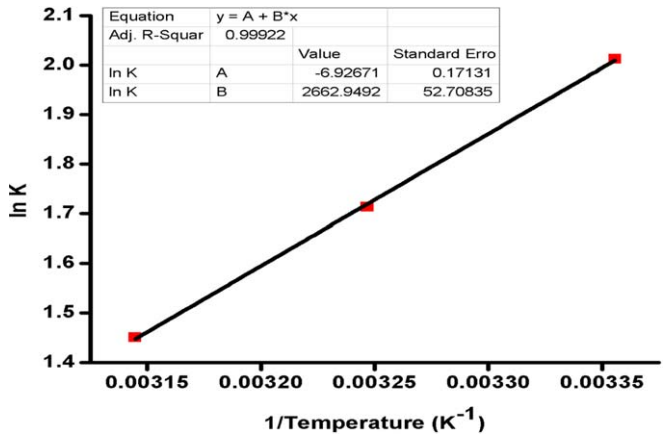

Figure 8. Van't Hoff plot for adsorption of fluoride onto PHP biochar.

Table 2. Comparison of Langmuir adsorption capacity (q_{max}(mg/g)) of various adsorbents with PHP biochar for fluoride adsorption.

S. no.	Adsorbent	Langmuir adsorption capacity (q_{max}(mg/g))	Reference
1	SnO_2-activated carbon	4.60	[33]
2	Rice husk ash	2.91	[34]
3	K_2CO_3 activated cotton nut shells	2.47	[35]
4	Aluminium impregnated coconut fiber ash	3.2	[36]
5	La-modified activated alumina	6.70	[37]
6	Fe-Al-Ce nanoadsorbent	2.22	[38]
7	Activated bagasse carbon of sugarcane	1.15	[39]
8	Sawdust raw	1.74	[39]
9	Wheat straw raw	1.93	[39]
10	Pecan (Carya illinoinensis) nut shell carbon modified with egg-shells carbon	2.51	[40]
11	Cynodon dactylon-based activated carbon	4.62	[41]
12	alum sludge	5.39	[42]
13	Fe-modified zeolite	2.31	[43]
14	Charcoal	3.77	[44]
15	Zirconium(iv)-impregnated cashew nut shell carbon	2.23	[45]
16	Carbonized Rice husk	1.99	[46]
17	Algal Spirogyra	1.27	[47]
18	PHP Biochar	3.665	Present Study

where, R and T are universal gas constant (8.314 J $mol^{-1}\cdot K^{-1}$) and temperatures in Kelvin (K), respectively. K_{CF} (dimensionless) is the thermodynamic equilibrium constant for fluoride adsorption onto PHP biochar and calculated by using equation (10):

$$K_{CF} = \frac{C_{ad,eq}}{C_{eq}} \tag{10}$$

where $C_{ad,eq}$ (mg l^{-1}) and C_{eq}(mg l^{-1}) are the equilibrium concentration of Fluoride ions on PHP biochar after adsorption and equilibrium concentration of Fluoride ions in solution after adsorption, respectively. The linear plot between ln (K_{CF}) versus 1/T known as Van't Hoff plot (see figure 8), which was used to calculate thermodynamic parameters such as ΔH^0 and ΔS^0 .

From table 4, the value of change in Gibbs free energy (ΔG^0) was negative, which showed that the fluoride adsorption onto PHP biochar was spontaneous. It was observed that the values of Gibbs energy were decreased with increasing temperature, i.e., the adsorption of fluoride onto PHP biochar were suitable at low temperature. The value of enthalpy was also negative, which confirmed that the reaction was exothermic in nature. Negative values of entropy (ΔS^0) showed the decreased randomness at the solid (PHP biochar)-liquid (fluoride) interface during the adsorption process.

Table 3. Kinetic parameters values for adsorption of fluoride onto PHP biochar.

		Initial concentration of fluoride	
	Parameter	10 mg l^{-1}	20 mg l^{-1}
Pseudo-first-order	$q_{e,exp}$(mg/g)	1.102	2.003
	$q_{e,cal}$(mg/g)	1.402	2.549
	K_1 (min^{-1})	0.027	0.029
	R^2	0.923	0.957
Pseudo-second-order	$q_{e,exp}$(mg/g)	1.102	2.003
	$q_{e,cal}$(mg/g)	1.746	3.158
	K_2 (min^{-1})	$7.34^{*}10^{-3}$	$4.23^{*}10^{-3}$
	R^2	0.981	0.983

Table 4. Estimated values of thermodynamic parameters such as ΔG^0, ΔH^0 and ΔS^0 for adsorption of Fluoride onto PHP Biochar.

Temperature (°C)	ΔG^0 (kJ/mol)	ΔH^0 (kJ/mol)	ΔS^0 (J/mol·K)
25	−4.986	−22.139	−57.59
35	−4.386		
45	−3.835		

5. Conclusion

A cost effective adsorbent was prepared by waste peanut hull and used for adsorption of fluride ions. PHP biochar was prepared by pyrolyzeation in a tubular reactor and then further characterized using instrumental techniques. FTIR studies revealed that PHP biochar had funtion groups which were effctive for fluoride adsoption. SEM analysis varified that prepared adsorbent was highly porous in nature. Adsoption of fluoride ions onto the PHP biochar surface was varified by EDS analysis. Surface area and pore volume of PHP biochar was estimated by BET analysis. The batch experiments were carried out to optimize various effecting parameters like initial pH, contact time, PHP biochar adsorbent dose, initial concentration of Fluoride ion in solution, and reaction temperature and after the optimization of parameters, maximum removal efficiency of PHP biochar adsorbent was 88.21% for the 10 mg l^{-1} fluoride concentration at pH 7 with 8 g l^{-1} biochar dose. For the isotherm study, adsorption equilibrium data were linearly fitted with experimental data to explain the adsorption process and it was found that the Langmuir model best applied to the experimental data as compared to Freundlich isotherm. So, according to the Langmuir model, the adsorption of fluoride onto PHP biochar occurred by monolayer adsorption of the surface of biochar adsorbent. Kinetic study of the adsorption process reveals that the pseudo-second-order model best fitted with experimental data as compared to the pseudo-first-order model. Thermodynamic analysis results show that the adsorption of Fluoride onto PHP biochar adsorbent was a spontaneous, exothermic, and feasible process under experimental condition.

ORCID iDs

Vijay Laxmi Yadav https://orcid.org/0000-0003-2926-7406

References

[1] Adimalla N and Li P 2019 *Human and Ecological Risk Assessment: An International Journal* **25** 81–103
[2] Li P, He X, Li Y and Xiang G 2019 *Exposure and Health* **11** 95–107
[3] Rasool A *et al* 2018 *Environ. Geochem. Health* **40** 1265–81
[4] Chakraborti D *et al* 2016 *J. Trace Elem. Med. Biol.* **38** 33–45
[5] Yadav K K *et al* 2019 *Ecotoxicology and Environmental Safety* **182** 109362
[6] Bhatnagar A, Kumar E and Sillanpää M 2011 *Chem. Eng. J.* **171** 811–40
[7] De Gisi S, Lofrano G, Grassi M and Notarnicola M 2016 *Sustain. Mater. Technol.* **9** 10–40
[8] Ye C *et al* 2019 *Ecotoxicology and Environmental Safety* **180** 366–73
[9] Rojas-Mayorga C K, Bonilla-Petriciolet A, Silvestre-Albero J, Aguayo-Villarreal I A and Mendoza-Castillo D I 2015 *Appl. Surf. Sci.* **355** 748–60
[10] Islam M and Patel R 2011 *Chem. Eng. J.* **169** 68–77

[11] He Y, Zhang L, An X, Wan G, Zhu W and Luo Y 2019 *Sci. Total Environ.* **688** 184–98
[12] Paudyal H *et al* 2012 *Chem. Eng. J.* **195-196** 289–96
[13] Daifullah A A M, Yakout S M and Elreefy S A 2007 *J. Hazard. Mater.* **147** 633–43
[14] Choong C E *et al* 2020 *Chemosphere* **239** 124765
[15] Pongener C, Bhomick P C, Supong A, Baruah M, Sinha U B and Sinha D 2018 *Journal of Environmental Chemical Engineering* **6** 2382–9
[16] Araga R, Soni S and Sharma C S 2017 *Journal of Environmental Chemical Engineering* **5** 5608–16
[17] Singh S, Prasad Chakraborty J and Kumar Mondal M 2020 *Fuel* **259** 116263
[18] Narayan R, Meena R P, Patel A K, Prajapati A K, Srivastava S and Mondal M K 2016 *Environmental Progress & Sustainable Energy* **35** 95–102
[19] Saka C 2012 *J. Anal. Appl. Pyrolysis* **95** 21–4
[20] Prajapati A K and Mondal M K 2019 *Korean J. Chem. Eng.* **36** 1900–14
[21] Dhanasekaran P, Satya Sai P M and Gnanasekar K I 2017 *J. Fluorine Chem.* **195** 37–46
[22] Nehra S, Raghav S and Kumar D 2019 *Environmental Nanotechnology, Monitoring & Management* **12** 100264
[23] Dong Y, Gao M, Song Z and Qiu W 2020 *Chemosphere* **239** 124792
[24] Dixit S and Yadav V L 2019 Comparative Study of Polystyrene/Chemically Modified Wheat Straw Composite for Green Packaging Application *Polymer Bulletin* **1** 1–20
[25] Kumar P, Dixit S and Yadav V L 2019 Preparation of Hydrophilic Bentonite Grafted Mixed Matrix Polyvinylchloride Membrane With Superior Hydrophilicity *Rasayan Journal of Chemistry* **12** 707–18
[26] Dixit S and Yadav V L 2019 *J. Clean. Prod.* **240** 118228
[27] Kalidindi S, Vecha M, Kar A and Raychoudhury T 2016 *Water Science and Technology: Water Supply* **17** 115–24
[28] Khound N J and Bharali R K 2018 *Journal of Environmental Chemical Engineering* **6** 1726–35
[29] Bansiwal A, Thakre D, Labhshetwar N, Meshram S and Rayalu S 2009 *Colloids Surf., B* **74** 216–24
[30] Kumar N P, Kumar N S and Krishnaiah A 2012 *J. Chil. Chem. Soc.* **57** 1224–31
[31] Saw P K, Prajapati A K and Mondal M K 2018 *J. Mol. Liq.* **269** 101–9
[32] Srivastava S, Agrawal S B and Mondal M K 2016 *Korean J. Chem. Eng.* **33** 567–75
[33] Mohanta D and Ahmaruzzaman M 2018 *Journal of Environmental Chemical Engineering* **6** 356–66
[34] Bibi S, Farooqi A, Yasmin A, Kamran M A and Niazi N K 2017 *Int. J. Phytorem.* **19** 1029–36
[35] Mariappan R, Vairamuthu R and Ganapathy A 2015 *Chin. J. Chem. Eng.* **23** 710–21
[36] Mondal N K, Bhaumik R and Datta J K 2015 *Alexandria Engineering Journal* **54** 1273–84
[37] Cheng J, Meng X, Jing C and Hao J 2014 *J. Hazard. Mater.* **278** 343–9
[38] Su C-L, Chen L, Wang T-J, Yu L-X and Jin Y 2013 *Water Science and Technology: Water Supply* **13** 1309–16
[39] Yadav A K, Abbassi R, Gupta A and Dadashzadeh M 2013 *Ecol. Eng.* **52** 211–8
[40] Hernandez-Montoya V, Ramirez-Montoya L A, Bonilla-Petriciolet A and Montes-Moran M A 2012 *Biochem. Eng. J.* **62** 1–7
[41] Alagumuthu G, Veeraputhiran V and Venkataraman R 2011 *Hemijska Industrija* **65** 23–35
[42] Sujana M and Anand S 2011 *Desalination* **267** 222–7
[43] Sun Y, Fang Q, Dong J, Cheng X and Xu J 2011 *Desalination* **277** 121–7
[44] Tchomgui-Kamga E, Ngameni E and Darchen A 2010 *J. Colloid Interface Sci.* **346** 494–9
[45] Alagumuthu G and Rajan M 2010 *Chem. Eng. J.* **158** 451–7
[46] Deshmukh W S, Attar S and Waghmare M 2009 *Nature, Environment and Pollution Technology* **8** 217–23
[47] Mohan S V, Ramanaiah S, Rajkumar B and Sarma P 2007 *J. Hazard. Mater.* **141** 465–74